Original Research Article

Aquifer vulnerability assessment of groundwater in a basement complex geology using fuzzy analytical hierarchy process

Abstract

Groundwater which is found in aquifers is one of the most reliable sources of water supply and its quantity is as important as its quality. Various factors contribute to the increase in contamination of groundwater thereby limiting its use. Basement complex has been known to be more susceptible to contamination due to the nearness of the aquifers to the surface. The study was carried out to develop an aquifer vulnerability map of the area using fuzzy-analytical hierarchy process (FAHP). Vertical Electrical Sounding (VES) was adopted for the electrical resistivity survey using the Schlumberger array. A total of 72 parametric VES locations were occupied beside wells and boreholes in the study area. From the interpreted geophysical data obtained, three parameters namely; overburden thickness, longitudinal conductance and coefficient of anisotropy including slope and lithology from remote sensing and geological datasets were employed for the aquifer vulnerability assessment. The fuzzy-analytical hierarchy process was employed in assigning weights to the various parameters implemented for this research. . The aquifer vulnerability index of the study area was classified into five; very low, low, moderate, high and very high. The aquifer vulnerability map produced showed that high and very high aquifer vulnerability indiceswere observed to dominate majority of the study area. The model validated using correlation of the aquifer vulnerability index values and water quality index values via the receiver operating characteristics (ROC) curve showed 64 % accuracy. The result obtained showed that the method is effectual for the assessment of aquifer vulnerability in the study area.

Keywords: Aquifer Vulnerability; Geophysical Investigation; Fuzzy AHP; Groundwater

Introduction

Water is a crucial and irreplaceable substance for life on Earth, playing a fundamental role in various natural processes, ecosystems, and human activities. Its importance extends across multiple dimensions, encompassing ecological, biological, environmental, and societal aspects. Water that occurs underground in the cracks and voids of soil, sand, and rock and flows slowly through the geologic formation of these elements is referred to as groundwater [1](Yeh et al., 2015), and the geological formation called aquifers. The quantity of groundwater in any area depends majorly on the geologic formations of the environment. Basement complex is made up of heterogeneous crystalline rocks, dominantly gneiss, granite and charnockites. They are impermeable in nature and contain negligible groundwater resources [2] (Akintorinwa et al., 2020).The discontinuous nature of the basement aquifer system makes detailed knowledge of the subsurface geology, its weathering depth and structural disposition through geologic and geophysical investigations inevitable [3, 4] (Adiat et al., 2009;Jayeoba and Oladunjoye, 2013). Basement complex areas are known to be vulnerable to contaminants due to their near to ground protective capacity. They often lack thick layers of sedimentary rocks (overburden) that act as natural filters for contaminants thereby making allowing pollutants to easily infiltrate the fractured bedrock and reach the groundwater. Basement complex aquifers typically have limited recharge rates due to their low permeability. This can hinder the natural dilution and flushing of contaminants once they enter the groundwater system.

Aquifer vulnerability is the degree to which an aquifer is likely to be contaminated from various sources. Aquifer vulnerability concept can be intrinsic (natural) or and specific (integrated) vulnerability [5] (Gogu &Dassargues, 2000). Vulnerability assessment has been recognized for its ability to delineate areas that are prone to contamination than others as a result of anthropogenic activities on/or near the earth's surface [6, 7](Babiker et al. 2005; Wen et al. 2009). Over the years, several methods have been adopted to investigate how susceptible an area is to

contamination. Geophysics has been employed for so many years in detecting the availability, quality and quantity of groundwater [8, 9] (Omosuyi and Oyemola, 2012; Adelusi et al., 2014). Geophysical survey of the subsurface involves the measurement/establishment of geo-electric parameter such as layer resistivity (ρa), thickness and depth for each lithologic unit. Of the various methods which have been used for vulnerability assessment, physical method such as GOD which was developed by Foster [10] has been widely used for vulnerability assessment. It consists of three major parameters, groundwater occurrence, overlying lithology, and depth). DRASTIC is another widely used method for the assessment of vulnerability, it consists of seven hydrogeological parameters such as depth, net recharge, aquifer media, soil media, topography, impact of vadose zone and conductivity of aquifer.

Resistivity Method has the widest adoption in groundwater assessment among the various geophysical methods with its usefulness in bedrock delineation, lithological boundary differentiation and determination of structural trends. Vertical electrical sounding VES, which is a technique used in geophysical survey evaluate the subsurface geoelectric parameters. Geoelectric parameters derived from VES are used to delineate possible geologic features and hydrogeological characteristics relevant to aquifer vulnerability mapping. To get a precise and reliable aquifer vulnerability model, important factors that contribute to the vulnerability of groundwater needs to be considered. This is often achieved by assigning weights to different conditioning factors and integrating them using statistical and mathematical models to produce aquifer vulnerability maps. Common examples of the statistical and mathematical models are analytical hierarchy process (AHP), fuzzy analytical hierarchy process (FAHP), TOPSIS, Fuzzy TOPSIS, SWARA etc. Of all the modeling algorithms, the AHP is the most widely applied model for the evaluation of aquifer vulnerability. However, the traditional AHP works by crisp judgments and is accompanied by uncertainty, thus it cannot really reflect the human thinking style [11] (Kahraman et al. 2003). Due to the inherent inadequacies of the AHP, it was replaced by fuzzy AHP. The fuzzy AHP technique is an advanced analytical method which was developed from the traditional AHP. It is a combination of the fuzzy algorithm which is a mathematical tool and AHP which is a decision making tool and subjective method for analyzing qualitative criteria to weigh the alternatives. Van Laarhoven and Pedrycz [12] proposed the FAHP in other to solve the decision problems encountered in traditional AHP. Fuzzification helps to make the factors unidirectional based on their role, and AHP gives necessary weights of the factors. Therefore, combination of fuzzy and AHP makes the assessment logical and scientific [13](Sunil Saha et al., 2021). Besides, this method has an advantage of using expert opinion which is necessary for aquifer vulnerability assessment.

Groundwater though widely recognized as the most reliable and sustainable source of water, the rapid increase in urban development and growing population leading to an increase in pollution level keeps enhancing the susceptibility of groundwater to contamination. The growing demand for potable water supply has been a major challenge in Ado-Ekiti. Most homes depend on water from hand–dug wells whose overall yield and quality are influenced by the alternating wet and dry seasons among other factors. Tinuola and Owolabi ([14] observed an increase in environmental pollution with urbanization in Ekiti State. The highest percentage of pollution was reported in Ado-Ekiti, with an alert on possible health hazards to the residents. In Ado Ekiti, geophysical assessment has been done to either delineate the groundwater potential or aquifer vulnerability of the area. However, they are limited to specific areas in the study area. Abiola et al. [15] assessed the groundwater potential and overburden protective capacity covering major areas in Ado Ekiti. However, the population of Ado Ekiti has increased with a corresponding increase in the level of urbanization being the state capital thereby leading to increased level of contaminants. In rising up to this challenge, there is a need to evaluate the aquifer vulnerability of the groundwater in Ado Ekiti. This research work hereby adopted the use of fuzzy-analytical hierarchy process in assigning weights to the various parameters implemented for this research in other to develop a predictiveconceptual model for the generation of aquifer vulnerability map of Ado Ekiti using parameters obtained from the electrical resistivity method and geologic information.

Geology and hydrogeology of the study area

The study area is bounded between latitudes 7° 33’ 20’’ and 7° 41’20’’ N and longitudes 5° 10’40’’ and 5° 20’0’’ E. It sits on an undulating terrain, surrounded by hills and valleys, with the crystalline rocks of the basement complex contributing to the geological features of the area. Erosional processes have shaped the landscape, resulting in undulating terrain and exposed rock outcrops. River valleys and floodplains contain alluvial deposits, influenced by the erosional processes in the upland areas. The geological history of Ado Ekiti is deeply rooted in the Precambrian era, with basement rocks formed over millions of years through a combination of igneous and metamorphic processes. These basement complex rocks, formed over millions of years through intense heat and pressure, are generally low in porosity and permeability. This means they have limited spaces for water to store and pathways for it to flow. However, within these seemingly impermeable rocks exist fractures and fissures serving as conduits, allowing rainwater to infiltrate the ground and reach deeper zones where it accumulates as groundwater. The study area is underlain by lithologic units such as granite, gneiss and schist (Fig. 1). Four main lithologic units consisting of Migmatite Gneiss, Charnockite, Undifferentiated granite, gneiss and older granite, porphyritic granite and Biotite Hornblende granite characterize the study area.

The study area receives an average annual rainfall of around 1,200 millimeters (mm), with variations depending on the specific year and location within the city. The hilly terrain can influence rainfall patterns, with some areas receiving slightly more precipitation than others. Furthermore, the study area is characterized by several rivers and streams, with notable ones being the Ureje River, Elemi River, and Ogbese River. These water bodies contribute to the overall surface water availability in the city.

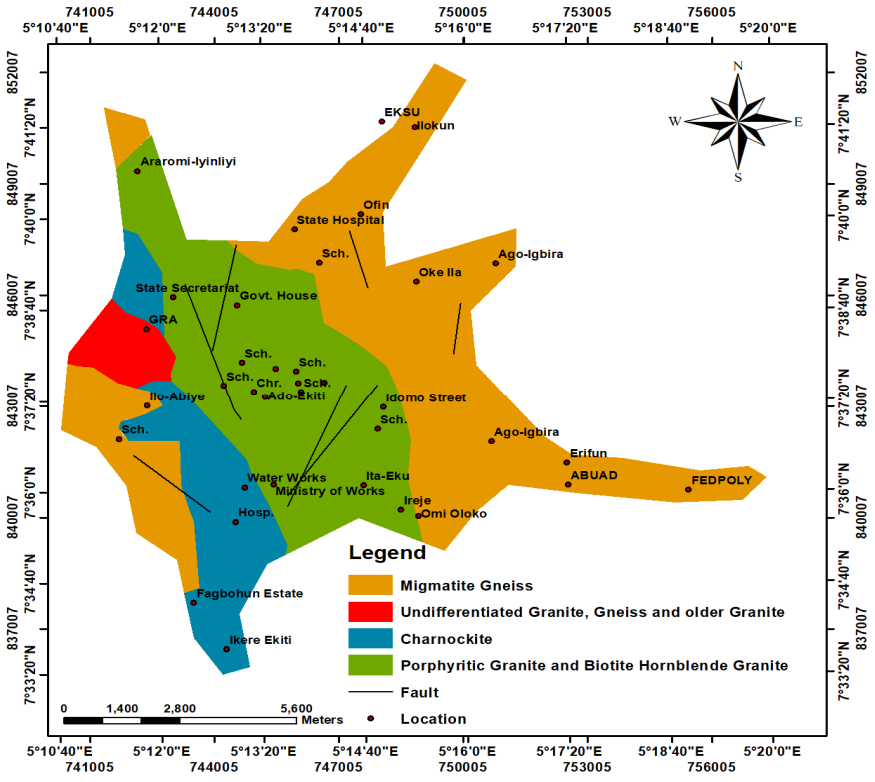

Fig 1: Geological Map of the Study Area

Research methodology

The Vertical Electrical Sounding (VES) was adopted for the electrical resistivity survey using the Schlumberger array. A total of 72 VES were carried out beside wells and boreholes in the study area. The electrode spacing (AB/2)

was varied between 1–100 m. The Ohm-mega resistivity meter was used in the data acquisition. The resistivity data were presented as field curves (by plotting the apparent resistivity (ρ_a) against AB/2 or half the spread length on a bi–logarithm paper) [16]. The data were interpreted qualitatively by visual inspection of the filed curves and quantitatively by partial curve matching with the use of master and auxiliary curves to obtain geoelectric parameters involving the initial estimates of resistivity values and thicknesses of various geoelectric layers at each VES point [17, 18](Zohdy and Jackson, 1965; Orellana and Mooney, 1966). These geoelectric parameters were used as initial starting models in the computer assisted iteration program (WinResist) to generate iterated curves when the field error is reduced as the field curve is matched with the model curve until a near to perfect fit is gotten [19, 20] (Keller and Frischnecht, 1966; Vander Velpen, 2004). The geoelectric parameters obtained from the resulting iterated curves were used to generate maps involving aquifer thickness, aquifer resistivity, overburden thickness, overburden resistivity, longitudinal conductance, coefficient of anisotropy and aquifer vulnerability of the study area.

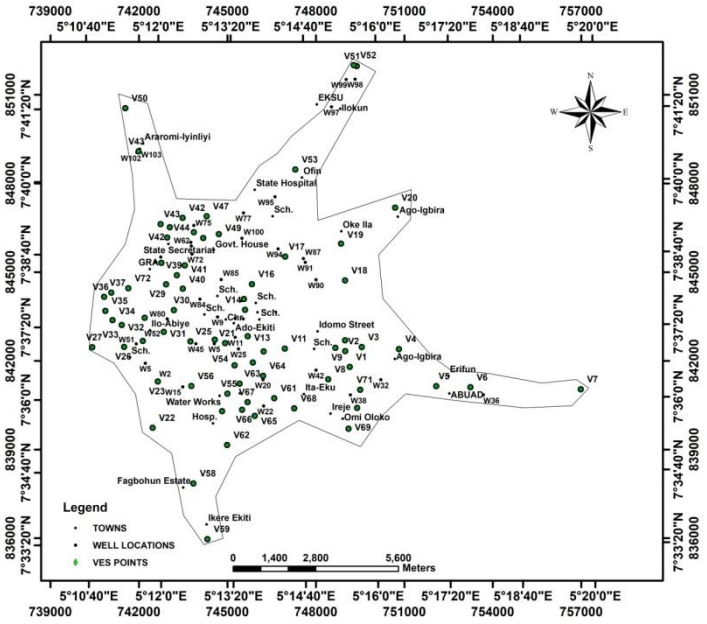

Fig 2: Base map of the Study Area Showing the VES Locations

Dar–Zarrouk Parameters (DZP)

The DZP is a secondary derived geo-electric parameter used for the further analysis of resistivity data obtained from the study area for the evaluation of the vulnerability of the aquifer in the study area to contamination. It is obtained using the first order geoelectric parameters involving layer resistivity values and thicknesses of geoelectric layers [21, 22] (Adiat *et al.*, 2020; Akinlalu*et al.*, 2021). The DZPs used in this study are the longitudinal conductance (L) and coefficient of anisotropy (λ)

Factors considered for vulnerability evaluation

The factors considered for evaluating how vulnerable the aquifer is to contamination are; overburden thickness, lithology, slope, longitudinal conductance and coefficient of anisotropy.

Lithology

Lithology which talks about the geology of an area plays a very vital role in the movement of water, as well as the percolation of contaminants into the aquifer. The lithology data was obtained from geological data in the literature.

Slope

Slope is the degree of steepness of an area. The slope of an area plays an important role in controlling the infiltration capacity of the soil [23](Chaudhry et al., 2019). If the value of slope is high, there is less infiltration of contaminants into the aquifer as a result of the high steepness and if the value of slope is low, there is a low possibility of the contaminants getting infiltrated into the aquifer. The slope of the study area was generated from the advanced spaceborne thermal emission and reflection radiometer (ASTER) digital elevation model (DEM) downloaded from www.earthexplorer.com. The digital elevation model of the study area was identified in three-dimensional (3-D) view from the ASTER DEM image. The slope map was produced from the ASTER DEM data and processed on ArcMap 10.7.2 software.

Longitudinal conductance

The longitudinal conductance (S) is the sum of all thickness/resistivity ratios of n–1 layers which overlie a semi–infinite substratum of resistivity ρ (eq. 1).

$$S = \sum_{i=1}^{N} \frac{h_i}{\rho_i} = \frac{h_1}{\rho_1} + \frac{h_2}{\rho_2} + \frac{h_3}{\rho_3} + \cdots + \frac{h_{n-1}}{\rho_{n-1}} \quad 1$$

It is used to assess the degree of clay content of subsurface lithology, serving as an aid in the determination of how susceptible an area is to pollution [24, 15, 22] (Oladapo *et al.*, 2004; Abiola *et al.*, 2009; Akinlalu*et al.*, 2021). This therefore means that the longitudinal conductance parameter interpretation gives the main natural protection of the granular and unconfined aquifers against contamination, related to the presence of overlapping clay layers, whose protection capability comes down to the infiltration time lag of solutions, due to their low permeability [25, 22](Adesola *et al.*, 2021; Akinlalu*et al.*, 2021). This essentially means that high longitudinal conductance values can be translated to high protective capacity of the aquifer unit in an area.

Coefficient of Anisotropy (COA) (λ)

The coefficient of anisotropy is also a second order geoelectric parameter derivation. Electrical coefficient anisotropy is a measure of the degree of the earth's inhomogeneity [26, 27](Billings, 1972; Maliek and Bhattacharya, 1973). It is essentially the square root of the ratio of the resistivity measured perpendicular to the bedding to that parallel to the bedding (eq.2). In a typical basement complex environment like the study area, this electrical effect is due to near surface features such as variable degree of weathering and structural features like faults, fractures, joints, foliations and beddings [28, 29, 21] (Ogungbemi*et al.*, 2013; Adiat *et al.*, 2018; Adiat *et al.*, 2020). These in turn are responsible for creating secondary porosity and effective porosity. These are important as regards groundwater accumulation and can also be used to determine the ease of contamination of aquifer units. It therefore means that an area with high coefficient of anisotropy is at a risk of being easily contaminated [21] (Adiat *et al.*, 2020).

The coefficient of anisotropy (λ) is given in equation 2 below

$$\lambda = \sqrt{\frac{\rho_t}{\rho_l}} = \sqrt{\frac{\sum_{i=1}^{n} \frac{h_i}{\rho_i} \sum_{i=1}^{n} h_i \rho_i}{\left(\sum_{i=1}^{n} h_i\right)^2}} \quad 2$$

Where $\rho_t$is the average traverse resistivity;

ρ_l is the average longitudinal resistivity;

h is the thickness of each geoelectric layer and;

ρ is the resistivity of each geoelectric layer.

Fuzzy analytical hierarchy process (FAHP)

Fuzzy-AHP was developed by Saaty [30] and it is a combination of two processes; fuzzy which is a mathematical tool and AHP which is a multi-criteria decision making method that makes a weighting judgment for issues. However, AHP has its limitation in the fact that it cannot comprise uncertainty for individual decisions which could be solved by fuzzy logic. This process is adopted to evaluate the parameters along with defining the fuzzy scores and weights of the coefficients [11] (Kahraman et al., 2004), which is then used to calculate the groundwater aquifer vulnerability index. The triangular fuzzy scale used in the FAHP weighting process expresses the importance of one factor over the other [31](Paksoy et al., 2012).

Table 1: Fuzzy scale [23] (Chaudhry et al., 2019)

Linguistic scale for the importance	Triangular fuzzy scale	Triangular fuzzy reciprocal scale
Just equal	(1,1,1)	(1,1,1)
Equally important	(1/2, 1, 3/2)	(2/3, 1, 2)
Weakly more important	(1, 3/2, 2)	(1/2, 2/3, 1)
Strongly more important	(3/2, 2, 5/2)	(2/5, 1/2, 2/3)
Very strongly more important	(5/2, 2,3)	(1/3, 1/2, 2/5)
Absolutely more important	(5/2, 3, 7/2)	(2/7, 1/3, 2/5)

The procedure used in the fuzzy-AHP is discussed in the following steps below:

Step 1: Calculating the fuzzy synthetic value (Si) in relation to the ith criterion.

$$Si = \sum_{j=1}^{m} M_{gi}^{j} \; x \; \left[\sum_{i=1}^{n} \sum_{j=1}^{m} M_{gi}^{j}\right]^{-1} \quad 3$$

To attain $\Sigma mj{=}1\ Mjgi$ given in equation (3), the fuzzy addition operator isperformed using equation (4).

$$\sum_{j=1}^{m} M_{gi}^{j} = \left[\sum_{j=1}^{m} l_j \sum_{j=1}^{m} m_j \sum_{j=1}^{m} u_j\right] \quad 4$$

Also, to attain, $[\sum ni{=}1\ \sum mj{=}1\ Mjgi] -1$ in equation (3), the fuzzy extension function for the values Mjgi (j=1, 2, ……., m) is computed as shown in equation (5).

$$\sum_{i=1}^{n} \sum_{i=1}^{m} M_{gi}^{j} = \left[\sum_{i=1}^{n} l_j \sum_{i=1}^{n} m_j \sum_{i=1}^{n} u_j\right] \quad 5$$

The following formula is used to obtain the inverse of equation (5).

$$\left[\sum_{i=1}^{n} \sum_{j=1}^{m} M_{gi}^{j}\right]^{-1} = \frac{1}{\sum_{i=1}^{n} u_1}, \frac{1}{\sum_{i=1}^{n} m_1}, \frac{1}{\sum_{i=1}^{n} l_1} \quad 6$$

Step 2: Calculating the degree of possibility (V) of two fuzzy numbers correspondingly, $M_2 = (l_2, m_2, u_2) \geq M_1 = (l_1, m_1, u_1)$ as follows-

$$V\ (2M_1) = supy{\geq}x\ [\ (\mu M_1\ (x), \mu M_2\ (y))] \quad 7$$

The connection between two fuzzy numbers M1 and M2 can be equally expressed as-

$$V(\ 2 \geq M_1) = \square gt(M_1 \cap M_2) = \mu M_2\ (d)$$

where the ordinate of the highest point of intersection D between M_1 and M_2 is denoted by d.

The values of both V ($M_1 \geq M_2$) and V (M2 ≥M1) are needed to compare M_1 and M_2.

Step 3: The degree to which a convex fuzzy number Mi (i = 1, 2, ……., k) can be greater than k is described by V (M ≥ M1, M2, ……., Mk).

$V\ [(MM1\ )andV\ (\ MM2\ )\ andV\ (\ MMk\ )$

$minV(\ \geq Mi\ )\ ,\ i$ = 1, 2, 3, …k 8

Let, $d1(\ A1\ )$ = min $V\ (\ S1 \geq Sk\ )$ 9

For k = 1, 2, ……., n where k ≠ i the weight vector can be expressed as,

$W\ '$ = $(d'\ (\ A1\ )\ ,\ (\ d'\ (\ A2\ )\ ,\ \ldots\ ..,\ d'\ (\ An\ ))T$ 10

Here, Ai (i= 1, 2, ……., n) are n elements.

Step 4: The normalized non-fuzzy weight W is determined after normalization as-

W = $(\ d\ (\ A1\ )\ ,\ (\ d\ (\ A2\ )\ ,\ \ldots,\ d\ (\ An\ ))T\ (\ An\ ))T$ (15)

where W is a nonfuzzy number

Table 2: Fuzzy pairwise comparison matrix and weight of the parameters

	Lithology	Overburden thickness	Coefficient of anisotropy	Longitudinal conductance	Slope
lithology	(1, 1, 1)	(1.5, 2, 2.5)	(1, 1.5, 2)	(0.5, 1, 1.5)	(2.5, 3, 3.5)
Overburden thickness	(0.4, 0.5, 0.67)	(1, 1, 1)	(0.67, 1, 2)	(0.5, 0.67, 1)	(0.5, 1, 1.5)
Coefficient of anisotropy	(0.5, 0.67, 1)	(0.5, 1, 1.5)	(1, 1, 1)	(0.67, 1, 2)	(1, 1.5, 2)
Longitudinal conductance	(0.67, 1, 2)	(1, 1.5, 2)	(0.5, 1, 1.5)	(1, 1, 1)	(2, 2.5, 3)
slope	(0.29,0.33,0.4)	(0.67, 1, 2)	(0.5, 0.67, 1)	(0.33, 0.4, 0.5)	(1, 1, 1)

Validation

Validation is an important aspect of assessing the predictive ability of any conceptual model [32](Akinlalu et al., 2024). To do this, aquifer vulnerability index values were compared with the water quality index derived from geochemical analyses of water wells in the investigated area via the receiver characteristics curve (ROC).

The ROC works by way of comparing the aquifer vulnerability index and water quality index values by evaluating the relationship between specificity and sensitivity of the data. Sensitivity is the proportion of the aquifers delineated with low vulnerability by evaluating the aquifer vulnerability index identified as positive on the curve while specificity is the proportion of the whole area under investigation with low vulnerability by evaluating the water quality index identified as negative on the curve. When the specificity and sensitivity equals 1, the false positive rate also equals 0. In this case, the ROC curve passes through the left hand corner of the plot, starting at the origin, and moves vertically to a sensitivity of 1 and horizontally to a positive rate of 1. The correlation between the aquifer vulnerability index and water quality index is then said to be perfect. However, rarely can a perfect correlation be attained. Hence, a correlation value greater than 0.5 using the ROC curve is believed to indicate a good correlation [33](Atenidegbe and Mogaji, 2023).

Results and discussions

The results of the geoelectric data presented in Table 3 shows a three, four and five layered geologic subsurface essentially characterizing the study area with HA, H, and A curves observed to be dominant. The curves show that the HA, H and A curves dominate the study area with 40%, 18% and 15% dominance respectively while others such as QHA, HAA, AA, AK, QH,AQ, KH, Q and K curves have 3%, 1%, 6%, 1%, 7%, 1%, 4%, 1%, and 1% occurrence respectively (Figure 3). The dominance of the HA, H and A curves is a strong indication of occurrence of hard rocks which are also close to the surface in the study area. The result of the geoelectric parameters showed that the study area is made up of three, four and five geoelectric layers with apparent resistivity values ranging from 7 to 15922 Ωm (Table 3). The geoelectric layers are designated as top soil, laterites, weathered/fractured basement and fresh basement.

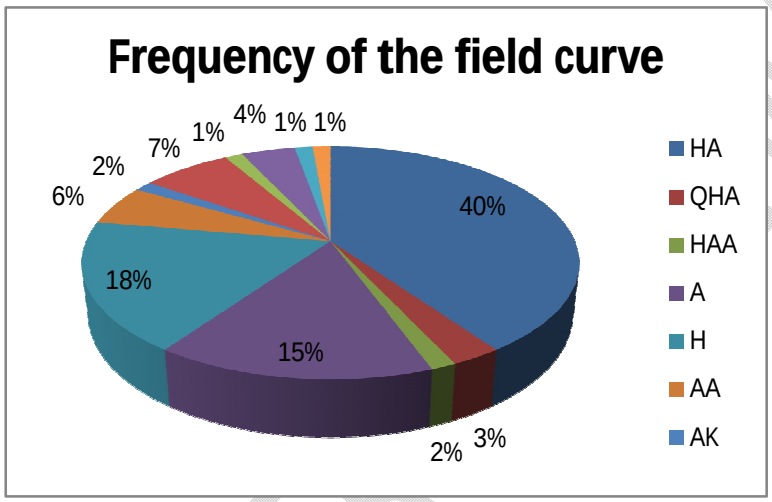

Figure 3: Pie Chart of the Frequency of the Field Curves in the Study Area.

Table 3: Summary of some geoelectric parameters and lithologic interpretation obtained in the study area

VES	Coordinate	RESISTIVITY (Ωm)	THICKNESS (M)	Lithology	CURVE TYPE
1	749150 841792	151	0.5	Top soil	HA
		35	4.5	Clay	
		266	8.7	Weathered basement	
		1395		Fresh basement	
2	748995 842328	255	0.5	Top soil	HA
		28	2.6	Clay	
		212	4.3	Weathered basement	
		1435		Fresh basement	
3	749557 842464	223	0.4	Top soil	HA
		10	2.9	Clay	
		196	4.2	Weathered basement	
		1568		Fresh basement	
4	750819 842398	329	1	Top soil	HA
		40	3.7	Clay	
		298	4.2	Weathered basement	
		998			

				Fresh basement	
		657	1.1	Top soil	
6	753240				QHA
	841102	117	1.7	Lateritic layer	
		38	4.8	Clay	
		282	5	Weathered basement	
		3306		Fresh basement	
		66	0.9	Top soil	
8	748422				HAA
	841374	35	1.6	Clay	
		79	5.3	Lateritic clay	
		219	10	Weathered basement	
		759		Fresh basement	
		89	0.8	Top soil	
10	748992				HA
	842694	20	4	Clay	
		197	4.3	Weathered basement	
		1982		Fresh basement	
		42	5.9	Top soil	
18	748990				AA
	844718	160	4.2	Lateritic clay	
		366	8.3	Weathered basement	
		1410		Fresh basement	
		129	3.3	Top soil	
22	742464				AK
	839733	651	2.3	Weathered basement	
		3937	15.4	Fresh basement	
		2326		Partially weathered basement	
		60	2.3	Top soil	
42	743483				KH
	846836	494	1.3	Lateritic layer	
		222	10.5	Weathered basement	
		994		Fresh basement	
		196	1	Top soil	
45	742733				QH
	846623	112	2.6	Lateritic clay	
		62	8.4	Weathered basement	
		1030		Fresh basement	
		243	5	Top soil	
50	744712				H
	846286	83	16.6	Weathered basement	
		461		Fresh basement	
		489	0.5	Top soil	
52	749389				QHA
	851968	227	1.7	Lateritic layer	
		30	6.6	Clay	
		202	7.3	Weathered basement	
		1349		Fresh basement	
		115	3	Top soil	
54	747305				Q
	848472	47	13	Weathered basement	

		25		Fractured basement	
55	745246	39	3	Top soil	A
	841848	166	12.6	Weathered basement	
		760		Fresh basement	

Table 3 (contd): Summary of some geoelectric parameters and lithologic interpretation obtained in the study area

VES	Coordinate	RESISTIVITY (Ωm)	THICKNESS (M)	LITHOLOGY	CURVE TYPE
56	744999	134	2.4	Top soil	KH
	840886	257	3.3	Lateritic layer	
		23	35.2	Weathered basement	
		172		Fresh basement	
57	743779	35	3.8	Top soil	A
	841146	379	10.9	Weathered basement	
		1756		Fresh basement	
59	743849	83	2.3	Top soil	K
	837852	1089	9.2	Fresh basement	
		402		Fractured basement	
63	744992	60	4	Top soil	H
	839150	40	8.8	Weathered basement	
		130		Fresh basement	
72	749506	391	1.1	Top soil	QH
	841020	115	5.7	Lateritic clay	
		39	11.5	Weathered basement	
		514		Fresh basement	

A CURVE TYPE

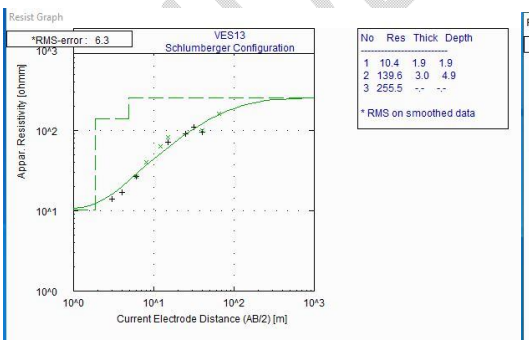

Q CURVE TYPE

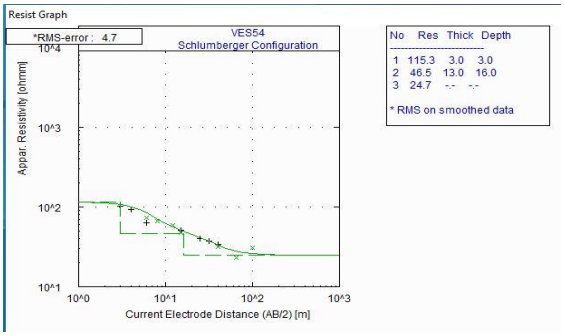

H CURVE TYPE **K CURVE TYPE**

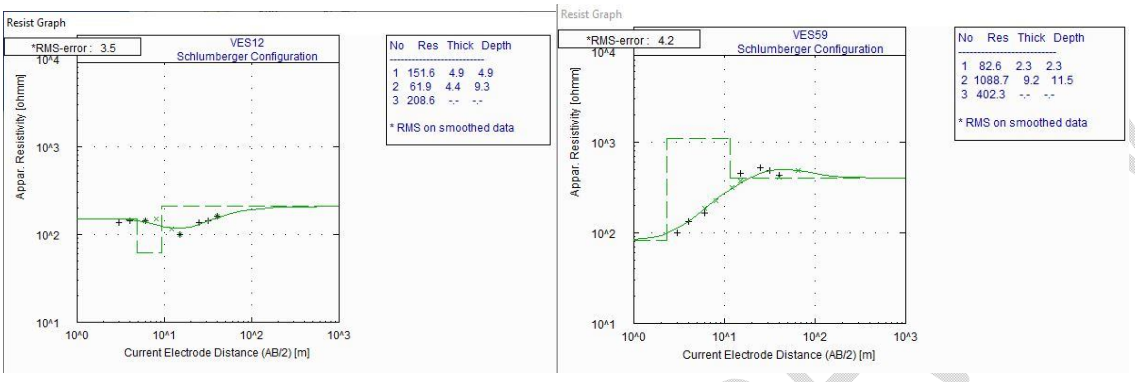

QHA AQ

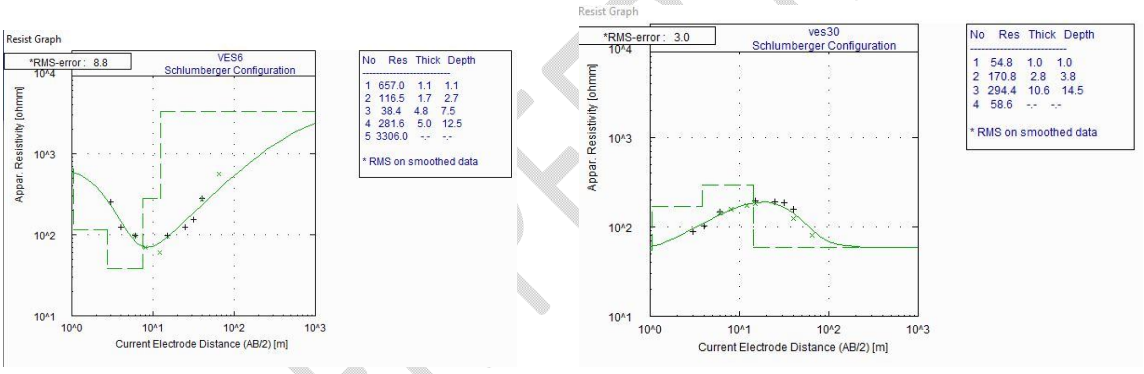

Fig 4: Some Representative Curve Types

Overburden Thickness

The overburden thickness derived from first order geoelectric data can be used to evaluate the vulnerability of the aquifer. A thick overburden decreases the rate of contamination of the aquifer unit below as it would reduce the time taken for fluids and contaminants to infiltrate into the aquifer. In the same vein, a thin overburden would increase the rate of contamination of the aquifer unit below as it will increase the rate of the recharge and passage of contaminants into the aquifer. This however, is dependent on the nature of the overburden. This means if the overburden has very low or very high resistivity values with thick overburden, the groundwater vulnerability of the aquifer unit would be effectively low. If however, the overburden is thin, the vulnerability of the aquifer to contamination will increase with time. Conversely, if the overburden has moderate resistivity values with thick overburden, the groundwater vulnerability of the aquifer to contamination will be low.

The study area generally has a thin overburden in the range of 0.5–24.0 m (Figure 5). Very thin overburden in the range of 0.5–3.3 m is observed in the central part extending to the eastern, western and northern flanks, occupying majority of the study area with conspicuous evidence around Odo-Ado, NTA road, Moferere, Ago Igbira, and Idemo street. The groundwater potential and aquifer vulnerability is expected to be very low considering the nature of the

overburden and the thin overburden, but the aquifer vulnerability should be expected to increase significantly over time in the shortest possible period.

Relatively thick overburden in the range of 7.9–24.0 m (Figure 5) is observed in the southern and northern flanks of the study area. The groundwater aquifer vulnerability is expected to be relatively low due to the impermeable nature of the overburden materials and the relative thickness of the overburden in the area. It is however, important to note that the aquifer vulnerability of the aquifer in the regions is subjective in the study area as the aquifer vulnerability may increase with time owing to the relatively thick overburden which is still quite thin.

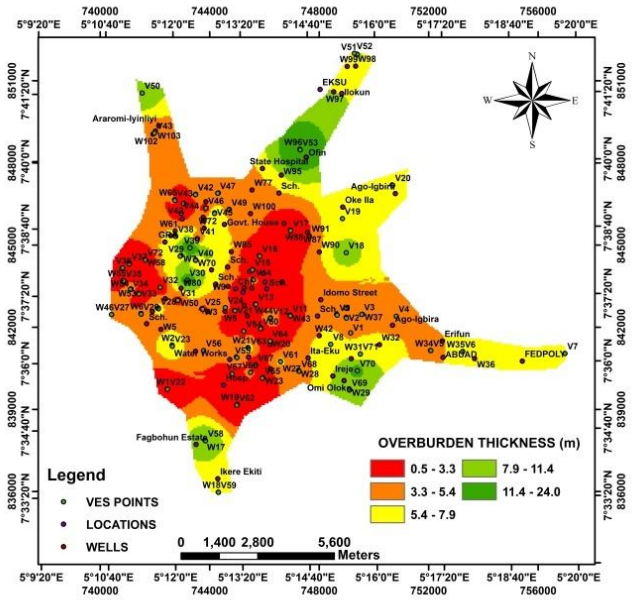

Fig 5: Overburden Thickness Map of the Study Area

Longitudinal Conductance

Longitudinal conductance is a second order geoelectric parameter and is used as a metric in analyzing the aquifer vulnerability of the study area. In explicit term, an overlying layer with high longitudinal conductance (generally greater than 1) [22](Akinlalu*et al.,* 2021) offers a high protection degree to contamination based on the relatively high thickness and low resistivity of the overlying strata [34] (Braga *et al.*, 2006).

The longitudinal conductance map of the study area shows the longitudinal conductance values range from 0.0027 - 0.8551 Ω^{-1} (Figure 6). The range of the longitudinal conductance values shows the area is greatly susceptible to groundwater contamination as the maximum longitudinal conductance value is less than 1. This is in part caused by the thin overburden observed across the study areas even in areas where the overlying strata has resistivity values to be very low as a result of the clayey formation present there (Figures 5). However, relatively high conductance values in the range of 0.3945 and 0.862 Ω^{-1} is mainly observed in patches around the central part of the study area indicated by green coloration. These areas have low resistivity (presence of clay units) with relatively considerable thickness. The aquifer vulnerability in these areas will be low because of the relatively high longitudinal conductance values, but the aquifer vulnerability cannot be assured on the long run owing to the relatively low overburden thickness in the area (Figure 5). Other areas having green, light green, yellow and red coloration are at a great risk of aquifer contamination because of the very low longitudinal conductance values in the range of 0.0027–0.3945 Ω^{-1} observed in those areas.

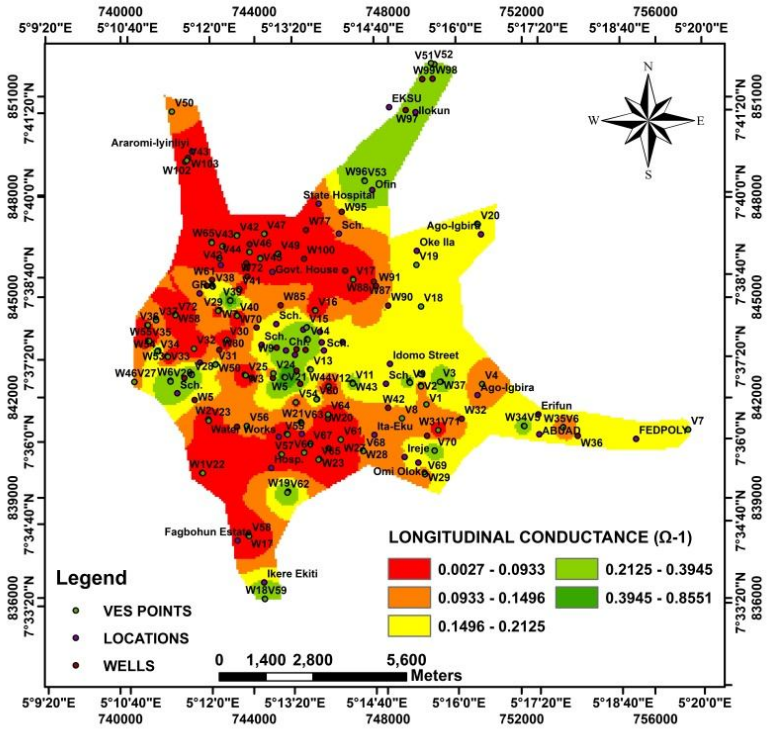

Fig 6: Longitudinal Conductance Map

Coefficient of Anisotropy

Coefficient of anisotropy is a second order geoelectric parameter and is used to evaluate the degree of heterogeneity in terms of weathering and existence of structural features of faults, fractures, joints, foliations etc. in the study area. According to Adiat *et al.* [29], coefficient of anisotropy values in the range of 2.31–2.64 is considered very high while 1.0–1.28 is considered very low. The coefficient of anisotropy map shows values in the range of 0.0833 and 2.1644 (Figure 7). High coefficient of anisotropy is observed as patches in the central and western flanks of the study area around V22, V58, and V17. This indicates that the areas are highly fractured and weathered, allowing the passage of fluids to the aquifer and also the contamination of the aquifer. This could be responsible for the low resistivity values possibly caused by contamination observed in some of the areas especially in the western part of the study area. Furthermore, very low coefficient of anisotropy in the study area indicated by green, light green to amber coloration in different parts of the study area is an indication of reduced weathering, fracturing causing reduced effective porosity and low groundwater potential and aquifer vulnerability. However, aquifer vulnerability evaluation is not dependent on the coefficient of anisotropy alone, as there can be absence of structural features and still be contamination of the aquifer units depending on the overlying materials on the aquifer.

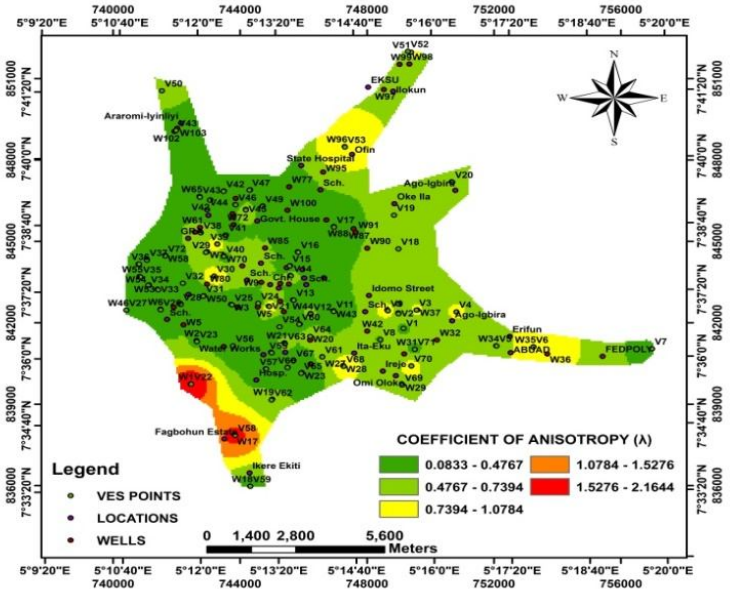

Fig 7: Coefficient of Anisotropy Map

Lithology

The fuzzified lithologic map of the study area recorded fuzzy score which ranged from 0.0 to 0.969 (Figure 8). Very high fuzzy scores represented by yellow and red color band are seen to dominate the porphyritic granite and hornblende granite and undifferentiated granite, gneiss and older granite region of the study area. This signature represents lithologic units in the study area that increases the risk of the contamination of the aquifer within them basically because of their weathering products and their degree of fracturing. These lithologic units are easily weathered and fractured when subjected to tectonism compared to other lithologic units in the study area. This means that contaminants can easily percoloate through them and find their way to aquifer units within the lithologic units. Very low fuzzy scores are represented by deep and light green (Figure 8), this signature represents lithologic units in the study area that decreases the vulnerability of the aquifer units. These lithologic units are essentially composed of Charnockite and migmatite gneiss. These lithologic units have a mix of low and very high resistivity values indicating that they are impermeable, and therefore, will not permit the migration of contaminants to aquifer units.

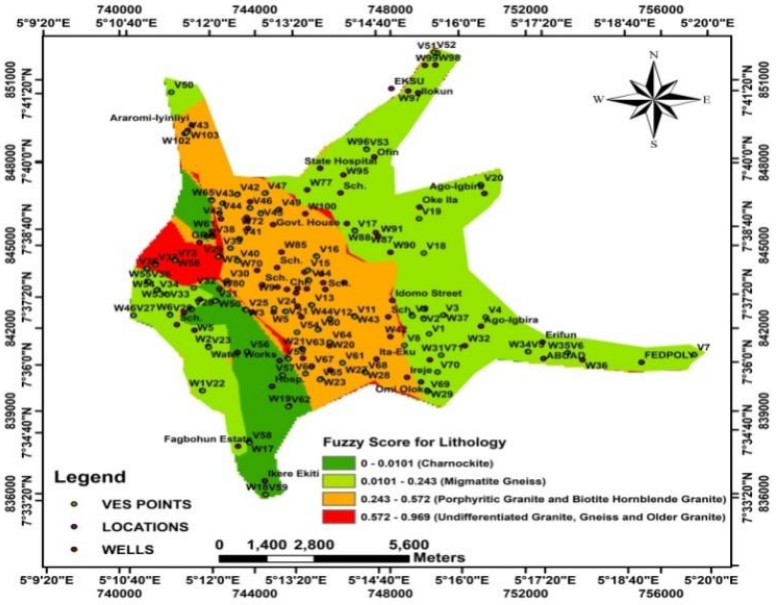

Fig 8: Fuzzified Lithology Map

Slope

Figure 9 shows the slope map of the study area with slope values in the range of 0^0–66.57^0 (Figure 9). The study area is almost entirely dominated by low to moderate slope in the range of 0^0–13.31^0, indicating that the topography of the study area is gentle. This type of topographic feature will allow gradual flow of the fluids and accumulation of fluids at a point. Subsequently, fluids including contaminants will find their ways to aquifer units through percolation. This therefore means that majority of the study area is at risk of contamination as a result of the gentle slope of the study area. Areas having slope values in the range of 13.31^0–66.57^0 are observed to have major occurrences in the central and northern parts of the study area. This represents areas of high slope, indicating the degree of steepness is high. These parts of the study area will not permit the percolation of fluids into the aquifer units, as the resident time for the percolation of fluids to the aquifer will be reduced due to the increase in runoff in the area as a result of the steepness of the slope.

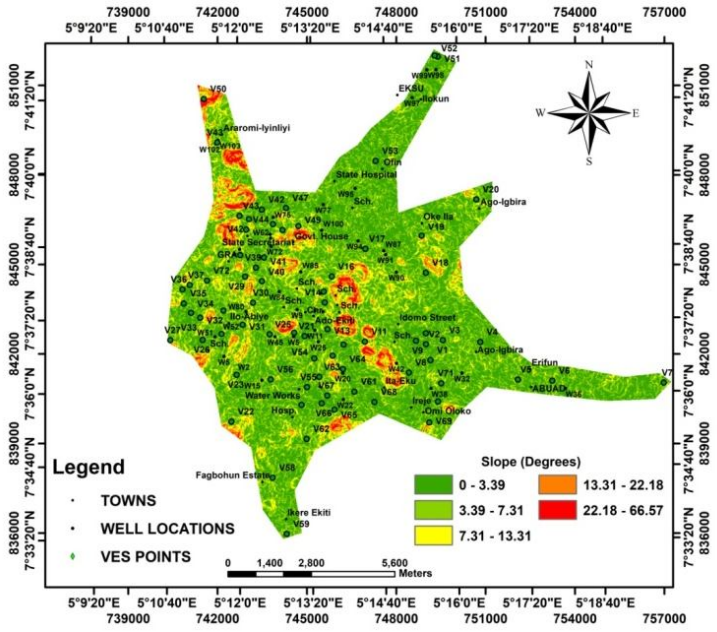

Fig 9: Slope Map of the Study Area

Aquifer Vulnerability Map

The aquifer vulnerability map of the study area was produced by integrating longitudinal conductance, coefficient of anisotropy, lithology and slope using the fuzzy gamma operator, 0.9. The aquifer vulnerability map (Figure 10) shows the aquifer vulnerability index of the study area with five classifications based on the degree of vulnerability using the natural break Jenk classification of the ArcMap 10.3 software. These classifications are very low, low, moderate, high and very high. High and very high aquifer vulnerability indices represented with amber and red coloration respectively are observed to dominate majority of the study area especially in regions around the eastern part, with minor occurrences in the northern part of the study area. This is a strong indication of the high vulnerability of the areas to aquifer contamination and is a strong expression of the high coefficient of anisotropy, low longitudinal conductance (moderate resistivity values and low overburden thickness), high fuzzy scores of lithology and low slope values. This explains why low resistivity values were observed over some aquifer units in the area arisen possibly from contamination. Very low to moderate aquifer vulnerability index is observed as patches interjecting the occurrences of high and very high aquifer vulnerability index in the study area. This anomaly has strong expression in the central and western parts of the study area, and this showed that the aquifer units in the areas are not susceptible to contamination because of the presence of the protective capacity of materials overlying the aquifer, coupled with the absence of structural features that could aid the migration of contaminants.

Table 4: Class scores and weight values of the main criteria influencing the aquifer vulnerability

Main Criteria	Classes	Class Score	Weights
Coefficient of Anisotropy (COA)	0.0833 – 0.4767	5	0.1938
	0.4767 – 0.7394	4	
	0.7394 – 1.0784	3	
	1.0784 – 1.5276	2	
	1.5276 – 2.1644	1	
Overburden Thickness (OVT)	0.5 – 3.3	5	0.1408
	3.3 – 5.4	4	
	5.4 – 7.9	3	
	7.9 – 11.4	2	
	11.4 – 24.0	1	

Lithology (Lith)	0 – 0.0101	1	
	0.0101 – 0.243	2	0.3171
	0.243 – 0.572	3	
	0.572 – 0.969	4	
	0 – 3.39	5	
Slope (S)	3.39 – 7.31	4	0.0818
	7.31 – 13.31	3	
	13.31 – 22.18	2	
	22.18 – 66.57	1	
	0.0027 – 0.0933	5	
Longitudinal Conductance (LC)	0.0933 – 0.1496	4	0.2665
	0.1496 – 0.2125	3	
	0.2125 – 0.3945	2	
	0.3945 – 0.8551	1	

Overlay of the geological map and the vulnerability map of the study area shows that areas of high vulnerability index coincide spatially with areas of Migmatite Gneiss, porphyritic Granite and Biotite Hornblende Granite in the central and eastern flank of the study area (Figure 11). This is majorly because these lithologies easily undergo weathering and fracturing under tectonism. Furthermore, the flaky feature of the Biotite Hornblende Granite makes it to undergo weathering easily under intense temperature and pressure to form clay. The formed clay being porous and not permeable would not permit the effective percolation of fluids and contaminants to aquifers. Coincidence of low aquifer vulnerability with the occurrence of Biotite Hornblende Granite is because of the presence of residual minerals such as Quartz and Muscovite, making them to be resistant to be weathering. It is generally observed that areas of low vulnerability have spatial relationship with Charnockite, undifferentiated Granite, older Granite and Gneiss in the study area. This is because Charnockite weathers to clay which is impermeable to the flow of fluids, hence, preventing contamination of the aquifer units. Also, the undifferentiated Granite, older Granite and Gneiss are mostly impervious, preventing the percolation of contaminants to the aquifer units.

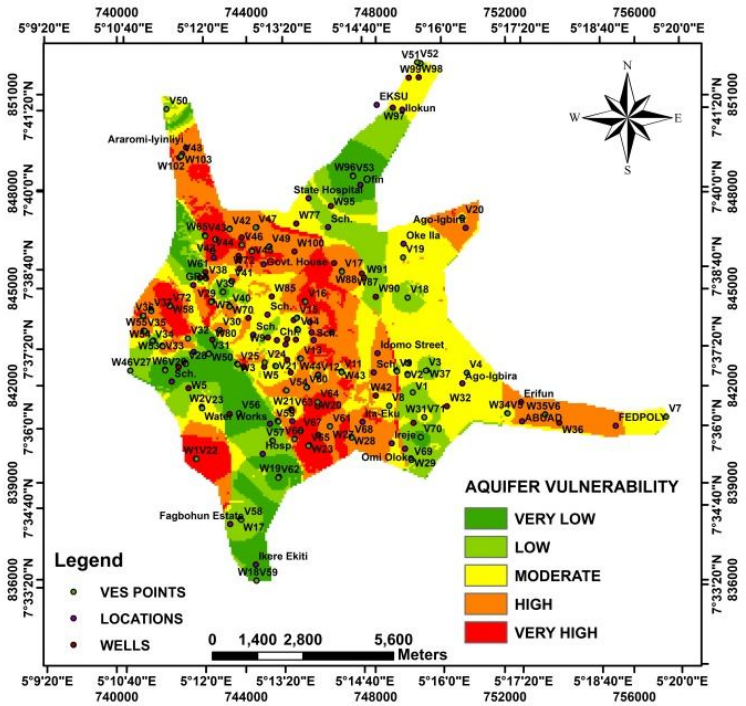

Fig 10: Aquifer Vulnerability Map of the Study Area

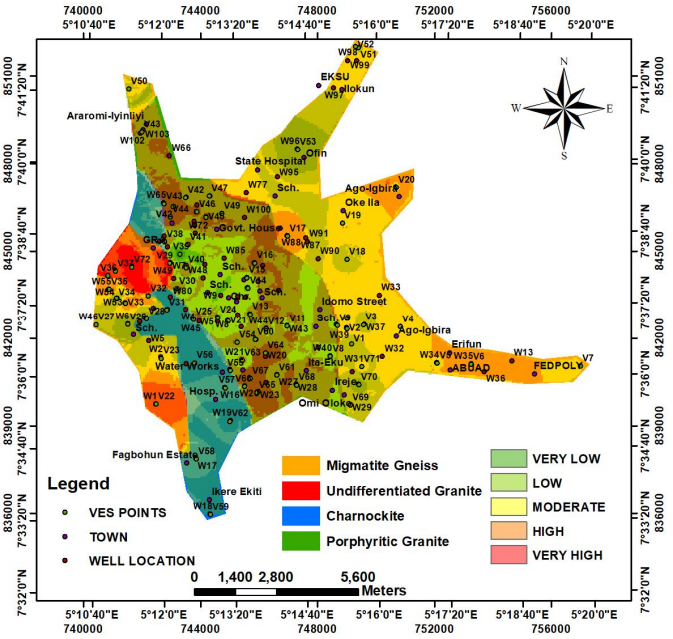

Fig 11: Overlay of Geological Map and Aquifer Vulnerability Map of the Study Area

Validation of model

To validate the accuracy of the fuzzy-AHP, the receiver operating characteristics (ROC) curve was employed. The quantitative validation of the aquifer vulnerability map using the ROC gave a prediction rate of 0.64 translating to a prediction accuracy of 64 % (Figure 12). This suggests that there is almost a perfect correlation between the aquifer vulnerability index derived from FAHP and water quality index. This further shows that the employed model produced by the Fuzzy-AHP is effectual, and suitable for aquifer vulnerability assessment.

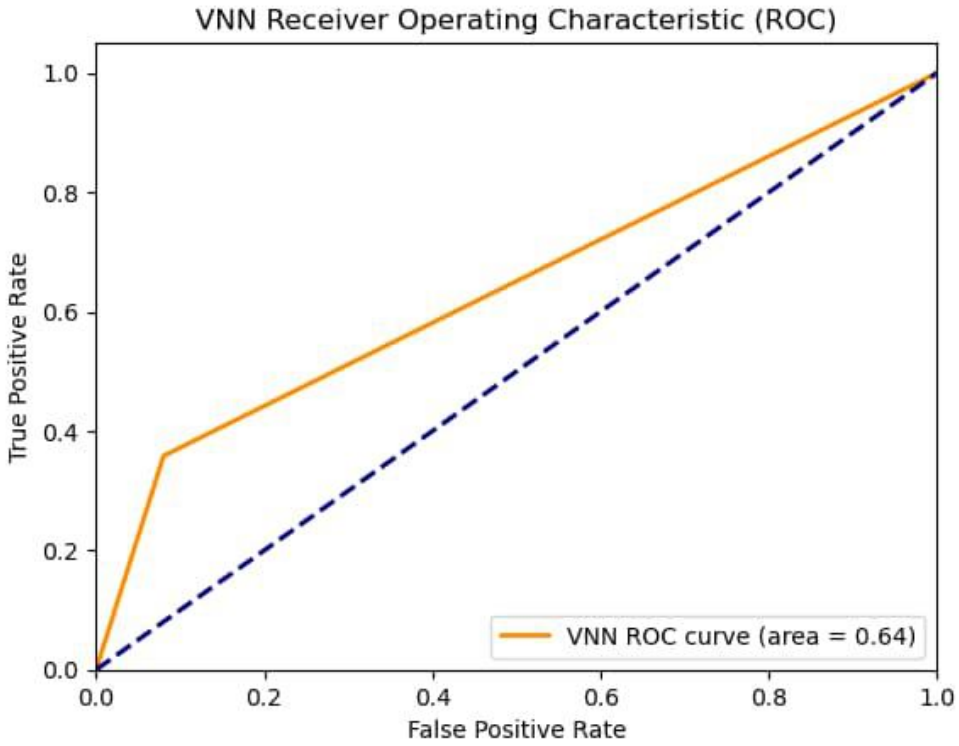

Fig 12: Quantitative validation using Area under the Curve (AUC) for Aquifer Vulnerability Map

Conclusion

The environmental problems associated areas with basement complex geology prompted the aquifer vulnerability assessment of groundwater in Ado-Ekiti. The research aimed to develop a conceptual model for the generation of aquifer vulnerability map of the study area. To achieve this, fuzzy analytical hierarchy process was employed toassign weights to the various parameters implemented. Electrical resistivity method was used to evaluate the subsurface parameter and the geoelectric parameters derived from VES were used to delineate possible geologic features and hydrogeological characteristics relevant to aquifer vulnerability mapping. The result obtained showed that the area is characterized by three to five geo-electric layers with the HA, H, and A curves observed to be dominant. Five geologic and subsurface parameters were considered for the aquifer vulnerability assessment; lithology, slope, overburden thickness, longitudinal conductance, and coefficient of anisotropy. The aquifer vulnerability index of the study area was classified into five; very low, low, moderate, high and very high. High and very high aquifer vulnerability indiceswere observed to dominate majority of the study area especially in regions around the eastern part, with minor occurrences in the northern part of the study area. Overlay of the geological map and the vulnerability map of the study area shows that areas of high vulnerability index coincide spatially with areas of migmatite gneiss, porphyritic granite and biotite hornblende granite in the central and eastern flank of the study area. The quantitative validation of the model using ROC by evaluating the correlation of the actual data and predicted data established that the model prediction accuracy was 64.0% suggesting that the model is suitable for predictive assessment of aquifer vulnerability in the study area and similar geologic environment.

References

1. Yeh, H.F., Cheng, Y.S., Lin, H.I., Lee, C.H., 2015. Mapping groundwater recharge potential zone using a GIS approach in Hualian River. Taiwan. Sustainable Environment Research doi:10.1016/j.serj.2015.09.005
2. Akintorinwa, O. J., Atitebi, M. O., &Akinlalu, A. A. (2020). Hydrogeophysical and aquifer vulnerability zonation of a typical basement complex terrain: A case study of Ododе Idanre southwestern Nigeria. *Heliyon*, *6*(8).
3. Adiat, K. A. N., Olayanju, G. M., Omosuyi, G. O., &Ako, B. D. (2009). Electromagnetic profiling and electrical resistivity soundings in groundwater investigation of a typical Basement Complex-a case study of Oda Town Southwestern Nigeria. *Ozean Journal of Applied Sciences*, *2*(4), 333-359.
4. Jayeoba, A., &Oladunjoye, M. A. (2013). Hydro-geophysical evaluation of groundwater potential in hard rock terrain of southwestern Nigeria. *RMZ Mater. Geoenviron*, *60*, 271-285.
5. Gogu, R. C., &Dassargues, A. (2000). Current trends and future challenges in groundwater vulnerability assessment using overlay and index methods. *Environmental geology*, *39*, 549-559.
6. Babiker, I. S., Mohamed, M. A., Hiyama, T., & Kato, K. (2005). A GIS-based DRASTIC model for assessing aquifer vulnerability in Kakamigahara Heights, Gifu Prefecture, central Japan. *Science of the Total Environment*, *345*(1-3), 127-140.
7. Wen, X., Wu, J., & Si, J. (2009). A GIS-based DRASTIC model for assessing shallow groundwater vulnerability in the Zhangye Basin, northwestern China. *Environmental Geology*, *57*, 1435-1442.
8. Omosuyi, G. O., &Oyemola, I. O. (2012). An assessment of hydrogeologic characteristic of Bamikemo's hard rock terrain using geophysical techniques. *Int J Water Resour Environ Eng*, *4*(5), 120-133.
9. Adelusi, A.O., Ayuk, M.A., Kayode, J.S., 2014. VLF-EM and VES: an application to groundwater exploration in a Precambrian basement terrain SW Nigeria. Ann. Geophys. 57 (1), 1–11. S0184
10. Foster, S. S. D. (1987). Fundamental concepts in aquifer vulnerability, pollution risk and protection strategy.
11. Kahraman, C., Cebeci, U., &Ulukan, Z. (2003). Multi□criteria supplier selection using fuzzy AHP. *Logistics information management*, *16*(6), 382-394.
12. Van Laarhoven, P. J., &Pedrycz, W. (1983). A fuzzy extension of Saaty's priority theory. *Fuzzy sets and Systems*, *11*(1-3), 229-241.
13. Sunil Saha, Barnali Kundu, Gopal Chandra Paul, Kaustuv Mukherjee, Biswajeet Pradhan, Abhirup Dikshit, Khairul Nizam Abdul Maulud& Abdullah M. Alamri (2021). Spatial assessment of drought vulnerability using fuzzy-analytical hierarchical process: a case study at the Indian state of Odisha, Geomatics, Natural Hazards and Risk, 12:1, 123-153, DOI: 10.1080/19475705.2020.1861114
14. Tinuola, F. R., & Owolabi, J. T. (2007). Issues in Environmental Pollution in Ekiti State. *Res J. Appl Sci*, *2*(5), 544-547.
15. Abiola, O., Enikanselu, P. A., & Oladapo, M. I. (2009). Groundwater potential and aquifer protective capacity of overburden units in Ado-Ekiti, southwestern Nigeria. *International Journal of Physical Sciences*, *4*(3), 120-132.
16. Koefoed, O. (1979). Resistivity sounding on an earth model containing transition layers with linear change of resistivity with depth. *Geophysical Prospecting*, *27*(4), 862-868.
17. Zohdy, A. A. (1965). The auxiliary point method of electrical sounding interpretation, and its relationship to the Dar Zarrouk parameters. *Geophysics*, *30*(4), 644-660.
18. Orellana, Ernesto, and Mooney, H. M., 1966, Master tables and curves for vertical electrical sounding over layered structures: Madrid, Interciencia.
19. Keller, G. V., & Frischknecht, F. C. (1966). Electrical methods in geophysical prospecting.
20. Velpen, B. A. (2004). Win RESIST Version 1.0. *M. Sc Research Project. ITC, Deft, Netherlands*.
21. Adiat, K. A. N., Ajayi, O. F., Akinlalu, A. A., & Tijani, I. B. (2020). Prediction of groundwater level in basement complex terrain using artificial neural network: a case of Ijebu-Jesa, southwestern Nigeria. *Applied Water Science*, *10*, 1-14.
22. Akinlalu, A. A., Mogaji, K. A., &Adebodun, T. S. (2021). Assessment of aquifer vulnerability using a developed "GODL" method (modified GOD model) in a schist belt environ, Southwestern Nigeria. *Environmental Monitoring and Assessment*, *193*(4), 199.
23. Chaudhry, A. K., Kumar, K., & Alam, M. A. (2021). Mapping of groundwater potential zones using the fuzzy analytic hierarchy process and geospatial technique. *Geocarto International*, *36*(20), 2323-2344.

24. Oladapo, M. I., Mohammed, M. Z., Adeoye, O. O., & Adetola, B. A. (2004). Geoelectrical investigation of the Ondo state housing corporation estate Ijapo Akure, Southwestern Nigeria. *Journal of mining and geology*, *40*(1), 41-48.
25. Adesola, B. M., Abdul-nafiu, A. K., Adewale, A. A., Stephen, I., Omowonuola, A. F., Omang, B. O., ... & Isaac, A. (2021). Groundwater sustainability and the divergence of rock types in a typical crystalline basement complex region, Southwestern Nigeria. *Turkish Journal of Geosciences*, *2*(1), 1-11.
26. Billings, M., 1972. Structural Geology, 3rd ed. Prentice Hall, Englewood Cliffr. NJ. 1972.
27. Maliek, S. B., Bhattacharya, D. C., & Nag, S. K. (1973). Behavior of fractures in hard rocks–a study by surface geology and radial VES methods. *Geoexploration*, *21*, 529-556.
28. Ogungbemi, O. S., Badmus, G. O., Ayeni, O. G., &Ologe, Oluwatoyin (2013). Geoelectric Investigation of Aquifer Vulnerability within Afe Babalola University, Ado–Ekiti, Southwestern Nigeria. *IOSR Journal of Applied Geology and Geophysics*, *1*(5), 1-7.
29. Adiat, K. A. N., Osifila, A. J., Akinlalu, A. A., &Alagbe, O. A. (2018). Mining of geophysical data to predict groundwater prospect in a basement complex terrain of southwestern Nigeria. *Int J Sci Technol Res*, *7*(5), 1.
30. Saaty, T. L. (1980). The analytic hierarchy process (AHP). *The Journal of the Operational Research Society*, *41*(11), 1073-1076.
31. Paksoy, T., Pehlivan, N. Y., & Kahraman, C. (2012). Organizational strategy development in distribution channel management using fuzzy AHP and hierarchical fuzzy TOPSIS. *Expert Systems with Applications*, *39*(3), 2822-2841.
32. Akinlalu, A. A., Afolabi, D. O., & Sanusi, S. O. (2024). Knowledge-Driven Fuzzy AHP Model for Orogenic Gold Prospecting in a Typical Schist Belt Environment: A Mineral System Approach. *Earth Systems and Environment*, *8*(2), 221-263.
33. Atenidegbe, O. F., &Mogaji, K. A. (2023). Modeling assessment of groundwater vulnerability to contamination risk in a typical basement terrain using TOPSIS-entropy developed vulnerability data mining technique. *Heliyon*, *9*(7).
34. Braga, A. C. D. O., Malagutti Filho, W., & Dourado, J. C. (2006). Resistity (DC) method applied to aquifer protection studies. *Revista Brasileira de Geofísica*, *24*, 573-581.